

Weak Gravitational Lensing as a Method to Constrain Unstable Dark Matter

Mei-Yu Wang and Andrew R. Zentner

*Department of Physics and Astronomy, University of Pittsburgh, Pittsburgh, PA 15260 **

(Dated: October 15, 2018)

The nature of the dark matter remains a mystery. The possibility of an unstable dark matter particle decaying to invisible daughter particles has been explored many times in the past few decades. Meanwhile, weak gravitational lensing shear has gained a lot of attention as probe of dark energy, though it was previously considered a dark matter probe. Weak lensing is a useful tool for constraining the stability of the dark matter. In the coming decade a number of large galaxy imaging surveys will be undertaken and will measure the statistics of cosmological weak lensing with unprecedented precision. Weak lensing statistics are sensitive to unstable dark matter in at least two ways. Dark matter decays alter the matter power spectrum and change the angular diameter distance-redshift relation. We show how measurements of weak lensing shear correlations may provide the most restrictive, model-independent constraints on the lifetime of unstable dark matter. Our results rely on assumptions regarding nonlinear evolution of density fluctuations in scenarios of unstable dark matter and one of our aims is to stimulate interest in theoretical work on nonlinear structure growth in unstable dark matter models.

PACS numbers: 98.80.-k,95.30.Cq,95.35.+d,95.85.Kr

I. INTRODUCTION

A preponderance of evidence supports a picture in which $\sim 5/6$ of the mass density of the Universe resides nonbaryonic dark matter (reviews include Refs. [1–3]). The prevailing hypothesis is that the dark matter is an as yet undetected particle that survives as a relic from the hot, early Universe. An effort to identify the dark matter now proceeds on many fronts and the dark matter is currently constrained by direct searches (e.g., Refs. [4–8]), indirect searches (e.g., Refs. [9, 10]), and astronomical observations (e.g., Refs. [11–14]). In this paper, we explore the possibility of constraining invisible decays of the dark matter particle using forthcoming statistical measurements of weak gravitational lensing.

Limits on unstable dark matter have been considered by numerous authors in the recent literature [15–25]. Radiative decays are very strictly limited, with the best constraints yielding lifetime bounds of $\tau_{\text{DDM}} \gtrsim 10^7 H_0^{-1}$ [26–30]. Assuming decays to Standard Model neutrinos, the least detectable Standard Model particles, places mass-dependent limits as restrictive as $\tau_{\text{DDM}} \gtrsim 10^3 H_0^{-1}$, for dark matter particle masses near 10^2 GeV [24, 31], though constraints are strongly mass dependent. Cosmological tests provide an opportunity to constrain the stability of the dark matter independent of particle mass and the interactions of the decay products, and current cosmological limits on invisible dark matter decays imply that the lifetime for decays to relatively light products is $\tau_{\text{DDM}} \gtrsim 50 H_0^{-1}$ [17, 20–22, 25, 32].

We consider the possibility of improving model-independent constraints on the dark matter particle lifetime using forthcoming weak lensing data. Such inde-

pendent constraints would be most relevant to models of light dark matter (masses $\lesssim 10$ MeV to evade neutrino constraints) or dark matter sufficiently sequestered from the Standard Model (e.g., Refs. [18, 19, 33–35]) and may help improve or complement constraints of asymmetric dark matter models [31, 36, 37]. For concreteness, we consider constraints on dark matter lifetime in a benchmark model of a cold dark matter particle that undergoes two-body decay to light daughter particles with a lifetime tuned to be exceptionally large.

The primary constraint comes from scale- and redshift-dependence of the cosmological gravitational lensing power spectrum at $z \sim 0 - 3$ after normalizing the power spectrum of density fluctuations at $z \approx 1100$ via cosmic microwave background (CMB) measurements. A full exploration of possible constraints is difficult because the nonlinear evolution of structure in the Universe in such models has not been extensively studied. In our most conservative forecasts for what may be possible with forthcoming instruments, we find that utilizing only scales on which linear perturbative evolution should be useful ($\ell < 300$) and taking weak prior constraints on other cosmological parameters, forthcoming surveys may produce dark matter lifetime constraints that are, at minimum, competitive with contemporary, model-independent constraints. More aggressive priors expected from Planck CMB measurements improve upon these constraints by roughly a factor of two. We argue that utilizing the information that may be available from nonlinear evolution should improve upon these constraints by an order of magnitude. Our most aggressive forecasts, using information extending to scales $\ell \leq 3000$ and taking Planck CMB prior constraints on other cosmological parameters, suggest that constraints as strong as $\tau_{\text{DDM}} \gtrsim$ a few $\times 10^2 H_0^{-1}$ may be possible with a survey covering a large fraction of the sky, such as that planned by the Large Synoptic Survey Telescope (LSST)

*Electronic address: mew56+@pitt.edu, zentner@pitt.edu

[38] or Euclid [39]. Achieving reliable constraints from such measurements requires an understanding of nonlinear evolution in unstable dark matter models. The possibility of stringent constraints on decaying dark matter from astronomical imaging surveys should be strong motivation to study the nonlinear evolution of cosmic structure formation in such scenarios (see also Refs. [18, 19]).

We continue our manuscript with a discussion of weak lensing observables in § II. We describe our benchmark model for unstable dark matter and the evolution of cosmological perturbations in such a model in § III. We discuss nonlinear structure evolution and the two methods we use to estimate nonlinear evolution in § IV. We describe our methods for forecasting constraints on unstable dark matter in § V. This section also includes a summary of our fiducial cosmological model and our assumptions regarding prior constraints. We illustrate the effects of unstable dark matter on lensing observables and present our forecast limits on dark matter lifetimes in § VI. Finally, we summarize and discuss avenues for future work in § VII.

II. WEAK GRAVITATIONAL LENSING OBSERVABLES

We explore the utility of weak gravitational lensing measurements for constraining the stability of the dark matter. Our most robust forecasts derive from considerations of possible weak lensing measurements restricted to scales where linear perturbative evolution of the metric potentials remains useful. In this manner, our paper is very similar in spirit to that of Schmidt [40], who studied constraints on modified gravity from weak lensing statistics restricted to linear scales. However, we attempt to estimate possible improvements to the constraining power of weak lensing observables, provided that nonlinear evolution can be modeled robustly.

We consider the set of observables that may be available from ongoing and forthcoming large-scale galaxy imaging surveys to be the auto- and cross-spectra of lensing convergence from sets of galaxies in N_{TOM} redshift bins. The $N_{\text{TOM}}(N_{\text{TOM}}+1)/2$ distinct convergence spectra are

$$P_{\kappa}^{ij}(\ell) = \ell^4 \int dz \frac{W_i(z)W_j(z)}{H(z)D_A^6(z)} P_{\Psi-\Phi}(k = \ell/D_A, z), \quad (1)$$

where i and j label the redshift bins of the source galaxies. We take $N_{\text{TOM}} = 5$ and consider evenly-spaced bins in redshift from a minimum redshift of $z = 0$ to a maximum redshift of $z = 3$. In agreement with the study of Ma et al. [41], we find that finer binning is not required to maximize the constraining power of such surveys. Weak lensing as a cosmological probe has been discussed at length in numerous papers (a recent review is Ref. [42]). We give a brief description of our methods below, which are based on the conventions and notation in Ref. [43] (to which we refer the interested reader for details).

In Eq. 1, $H(z)$ is the Hubble expansion rate, D_A is the comoving angular diameter distance, and $P_{\Psi-\Phi}(k, z)$ is the power spectrum of Newtonian gauge scalar potentials $\Psi - \Phi$ at wavenumber k and redshift z . In the following section, we describe our use of the publicly-available **CMBFAST** code to calculate $P_{\Psi-\Phi}(k, z)$, in which case it will be more natural to work in the synchronous gauge. Transforming between coordinate systems can be accomplished straightforwardly by following, for example, the methods described in Ref. [44] which we do not repeat here.

The W_i are the so-called lensing weight functions for source galaxies in redshift bin i . In practice, the galaxies will be binned by photometric redshift, so that the bins will have nontrivial overlap in true redshift (see Ref. [41] for a detailed discussion). Defining the true redshift distribution of source galaxies in the i th photometric redshift bin as dn_i/dz , the window functions are

$$W_i(z) = D_A \int dz' \frac{D_A(z, z')}{D_A(z')} \frac{dn_i}{dz'} \quad (2)$$

where $D_A(z, z')$ is the angular diameter distance between redshift z and z' .

We model the increased uncertainty induced by utilizing photometric galaxy redshifts with the probability function of assigning an individual source galaxy photometric redshift z_p given a true redshift z , $P(z_p|z)$. In this notation, the true redshift distribution of sources in the i th photometric redshift bin is

$$\frac{dn_i(z)}{dz} = \int_{z_{p,i}^{(low)}}^{z_{p,i}^{(high)}} dz_p \frac{dn(z)}{dz} P(z_p|z) \quad (3)$$

Here we take the true redshift distribution to be

$$\frac{dn(z)}{dz} = \bar{n} \frac{4z^2}{\sqrt{2\pi z_0^3}} \exp[-(z/z_0)^2] \quad (4)$$

with $z_0 \simeq 0.92$, so that the median survey redshift to $z_{med} = 1$, and \bar{n} as the total density of source galaxies per unit solid angle [45–47]. We assume that uncertain photometric redshifts can be approximated by taking

$$P(z_p|z) = \frac{1}{\sqrt{2\pi}\sigma_z} \exp\left[-\frac{(z_p - z)^2}{2\sigma_z^2}\right] \quad (5)$$

where $\sigma_z(z) = 0.05(1+z)$ [41]. Complexity in photometric redshift distributions is something that must be overcome to bring weak lensing constraints on cosmology to fruition (e.g., Ref. [48, 49]).

Observed convergence power spectra $\bar{P}_{\kappa}^{ij}(\ell)$, contain both signal and shot noise,

$$\bar{P}_{\kappa}^{ij}(\ell) = P_{\kappa}^{ij} + n_i \delta_{ij} \langle \gamma^2 \rangle \quad (6)$$

where $\langle \gamma^2 \rangle$ is the noise from intrinsic ellipticities of source galaxies, and n_i is the surface density of galaxies in the i th tomographic bin. We follow the recent convention and

set $\sqrt{\langle\gamma^2\rangle} = 0.2$, subsuming additional errors on galaxy shape measurements into an effective mean number density of galaxies, \bar{n} . Assessments of intrinsic shape noise per galaxy may be found in, for example [38, 50, 51]. Assuming Gaussianity of the lensing field, the covariance between observables \bar{P}_κ^{ij} and \bar{P}_κ^{kl} is

$$C_{AB} = \bar{P}_\kappa^{ik} \bar{P}_\kappa^{jl} + \bar{P}_\kappa^{il} \bar{P}_\kappa^{jk} \quad (7)$$

where the i and j map to the observable index A , and k and l map to B such that C_{AB} is a square covariance matrix with $N_{\text{TOM}}(N_{\text{TOM}} + 1)/2$ rows and columns. We assume Gaussianity throughout this work and consider only multipoles $\ell < 3000$ at which point the Gaussian assumption and several weak lensing approximations break down [52–56].

III. PERTURBATION THEORY WITH UNSTABLE DARK MATTER

Our aim is to predict the power spectrum of weak gravitational lensing convergence in unstable dark matter scenarios. To do so, we must compute the modifications to the metric potentials in unstable dark matter scenarios [see Eq. (1)]. We explore a restricted set of models in which a massive parent dark matter particle decays into a significantly lighter pair of daughter particles. For the sake of specificity, we adopt a decaying dark matter (DDM) scenario in which massive majorana parent particles decay into relativistic daughter (RD) particles via two-body decay and use this scenario to benchmark observational constraints. In such a scenario, the lifetime of the unstable dark matter particle lifetime (τ) is the only nonstandard free parameter. One could assume decay to a combination of heavy and light daughter particles in which case the mass differences are important additional parameters that establish the recoil velocities of the decay product particles (as explored in detail in Refs. [18, 19], recently).

The distribution functions of DDM (f_{DDM}) and RD (f_{RD}) evolve according to the coupled Einstein-Boltzmann equations. In particular (e.g., [15, 44]),

$$\frac{df_{\text{DDM}}}{d\tau} = -\frac{a^2 m_{\text{DDM}}}{\tau_{\text{DDM}} \epsilon_{\text{DDM}}} f_{\text{DDM}} \simeq -\frac{1}{\tau_{\text{DDM}}} f_{\text{DDM}} \quad (8)$$

$$\frac{df_{\text{RD}}}{d\tau} = \frac{a^2 m_{\text{DDM}}}{\tau_{\text{DDM}} \epsilon_{\text{DDM}}} f_{\text{DDM}} \simeq \frac{1}{\tau_{\text{DDM}}} f_{\text{DDM}}, \quad (9)$$

where τ is the conformal time and τ_{DDM} , ϵ_{DDM} , and m_{DDM} are the lifetime, energy, and mass of decaying dark matter. Following established procedure, we express the distribution function of species X as a zeroth-order distribution plus a perturbation,

$$f_X(\vec{x}, \vec{q}, \tau) = f_X^0(q, \tau)[1 + \Psi_X(\vec{x}, \vec{q}, \tau)] \quad (10)$$

The evolution of the mean energy density for DDM and its RD particles follow from the zeroth-order integrals of

Eq. (8) and Eq. (9),

$$\dot{\rho}_{\text{DDM}} + 3H\rho_{\text{DDM}} = -\Gamma\rho_{\text{DDM}} \quad (11)$$

$$\dot{\rho}_{\text{RD}} + 4H\rho_{\text{RD}} = \Gamma\rho_{\text{DDM}} \quad (12)$$

Here and throughout, we designate \dot{y} as the time derivative of y , and we denote the decay rate as $\Gamma = 1/\tau_{\text{DDM}}$. In the limit of a massive DDM particle, evolution of the comoving density $\rho_{\text{DDM}} a^3$ approaches $\propto \exp(-t/\tau_{\text{DDM}})$.

The collision term describing the DDM decays is proportional to f_{DDM}^0 , rendering the equations describing the evolution of DDM perturbations identical to those of standard, stable cold dark matter at the lowest order in perturbation theory. The perturbation equations describing the daughter particles are less trivial. Following Refs. [15, 44], we expand the perturbation equations for RD particles in a series of Legendre polynomials $P_l(x)$, yielding

$$F_{\text{RD}}(\vec{k}, \hat{n}, \tau) = \frac{\int dq q^3 f_{\text{RD}}^0(q, \tau) \Psi_{\text{RD}}}{\int dq q^3 f_{\text{RD}}^0(q, \tau)} \\ = \sum_{l=0}^{\infty} (-i)^l (2l+1) F_{\text{RD},l}(\vec{k}, \tau) P_l(\hat{k} \cdot \hat{n}), \quad (13)$$

where $F_{\text{RD},l}(\vec{k}, \tau)$ are the harmonic expansion coefficients. The orthonormality of Legendre polynomials allows the evolution equations to be written as

$$\dot{\delta}_{\text{RD}} = -\frac{2}{3}(\dot{h} + 2\theta_{\text{RD}}) + \frac{\rho_{\text{DDM}}}{\rho_{\text{RD}}}(\delta_{\text{DDM}} - \delta_{\text{RD}}) \quad (14a)$$

$$\dot{\theta}_{\text{RD}} = k^2 \left(\frac{\delta_{\text{RD}}}{4} - \sigma_{\text{RD}} \right) - \frac{\rho_{\text{DDM}}}{\rho_{\text{RD}}} \theta_{\text{RD}} \quad (14b)$$

$$\dot{\sigma}_{\text{RD}} = \frac{2}{15}(2\theta_{\text{RD}} + \dot{h} + 6\dot{\eta} - \frac{9}{2}kF_{\text{RD},3}) \\ - \frac{\rho_{\text{DDM}}}{\rho_{\text{RD}}} \sigma_{\text{RD}} \quad (14c)$$

$$\dot{F}_{\text{RD}} = \frac{k}{2l+1} [lF_{\text{RD},l-1} - (l+1)F_{\text{RD},l+1}] \\ - \frac{\rho_{\text{DDM}}}{\rho_{\text{RD}}} F_{\text{RD},l}, \quad l \geq 3 \quad (14d)$$

at first order, where $\delta_{\text{RD}} \equiv F_{\text{RD},1}$, $\theta_{\text{RD}} \equiv 3/4kF_{\text{RD},1}$, $\sigma_{\text{RD}} \equiv F_{\text{RD},2}$, and h is the scalar trace of the metric perturbation, all in well-established notation.

We have modified the publicly-available CMBFAST code of Seljak and Zaldarriaga [57] to compute the potential power spectra. As we noted in § II, we quote the perturbation equations explicitly in synchronous gauge simply because CMBFAST is written in terms of the synchronous gauge perturbations. Gauge transformations can be made straightforwardly [44].

The growth of perturbation is affected by the change of energy density among the relativistic and nonrelativistic components. From Eq. (11) and Eq. (12) we can see

that in the decaying dark matter scenario the comoving dark matter density decreases exponentially, and all of this decrement is transferred into relativistic energy density. Consequently, perturbation growth exhibits a scale-dependent suppression relative to stable dark matter, where the relevant scale is the horizon size at the epoch of decay. This late-time suppression of structure growth in large part provides the necessary leverage for weak lensing constraints on unstable dark matter. For daughter particles, the additional ρ_{DDM}/ρ_{RD} terms have an impact on scales greater than the horizon at the time of decay [15].

As we will discuss below, some of the constraining power of weak gravitational lensing comes from observations made on scales where linear perturbation theory is no longer adequate (e.g., [40, 43, 52, 58–60]). The constraints we forecast in the following sections that are based on linear scales only are robust and interesting in and of themselves. However, the utility of weak lensing is greatly increased if scales modified by nonlinearity can also be exploited for cosmological constraints [43], so we explore multiple proposed nonlinear corrections to linear evolution in the following section.

IV. NONLINEAR EVOLUTION

In the standard application of weak lensing to constrain dark energy, most of the constraining power comes from scales on which linear evolution of cosmological perturbations is no longer valid. Accounting for nonlinear evolution enables a larger range of multipoles to be used, and nonlinear evolution greatly enhances signal-to-noise of weak lensing measurements at multipoles $\ell \gtrsim 300$. To estimate the constraints that may be anticipated from a full, nonlinear treatment of DDM, we explore nonlinear corrections to linear evolution using both the method of Smith et al. [61], and a halo model-inspired method by Peter [18]. Smith et al. [61] provide an empirical fit for nonlinear power given a linear power spectrum. We utilize the fit of Smith et al. [61] directly as one of our nonlinear structure models. This is not entirely unreasonable, because lifetimes of interest are far larger than a Hubble time, so little decay occurs relative to a standard cosmological model. We implement the method of Peter [18] using the halo model as follows.

The halo model (see Ref. [62] for a review) is based on the assumption that all matter resides within dark matter halos. The matter power spectrum is given by the sum of two terms,

$$P(k) = P_{1H}(k) + P_{2H}(k), \quad (15)$$

where

$$P_{1H}(k) = \frac{1}{\rho_M^2} \int dm m^2 \frac{dn}{dm} \lambda^2(k|m), \quad (16)$$

and

$$P_{2H}(k) = \frac{1}{\rho_M^2} P^{\text{lin}}(k) \left[\int dm m \frac{dn}{dm} \lambda(k|m) b_h(m) \right]^2. \quad (17)$$

In the foregoing equations, ρ_m is the mean matter density of the universe, m is halo mass, $\lambda(k|m)$ is the Fourier transform of the Navarro, Frenk, and White (NFW, Ref. [63]) density profile for a halo of mass m , $P^{\text{lin}}(k)$ is the linear matter power spectrum, and $b_h(m)$ is the halo bias function. The one-halo term $P_{1H}(k)$, describes correlations among mass elements within a common halo while the two-halo term $P_{2H}(k)$, is due to correlations among mass elements in distinct halos.

To estimate the impact of decaying dark matter on matter clustering, we follow the approach denoted as *Case 1* by Ref. [18] to describe modifications to the halo mass function, halo bias, and internal halo structure. We then incorporate these modifications into the halo model formulae of Eq. (16) and Eq. (17) to compute lensing power spectra. This model is based upon the assumption that halos at early times are very much like their counterparts in models of stable, cold dark matter (because little decay will occur in any viable model) and that modifications to halo structure can be described by the conservation of adiabatic invariants describing dark matter particle orbits.

Consider a population of dark matter halos that formed prior to any significant dark matter decays such that halos at any time $t \ll H_0^{-1}$ can be modeled as standard, CDM halos. These halos then lose mass as their constituent dark matter particles decay. If the decay lifetime is much larger than the halo dynamical timescale (as it will always be in cases of interest because dynamical times are $\tau_{\text{dyn}} \lesssim 0.1 H_0^{-1}$ and viable regions of parameter space are $\tau_{\text{DDM}} \gg H_0^{-1}$), then the halo gravitational potential changes adiabatically. Exploiting the adiabatic invariance of angular momentum for particles on nearly circular orbits, establishes a prediction for the relationship between the initial and final matter distribution within a dark matter halo,

$$M_i(r_i)r_i = M_f(r_f)r_f, \quad (18)$$

where $M_i(r)$ is the mass enclosed within radius r in the initial, early-time halo, $M_f(r)$ is the corresponding quantity describing the contemporary, late-time halo, and r_i and r_f are the initial and final radii of a particle shell, assuming that mass shells never cross and particles move in circular orbits. Eq. (18) is the basic relation of the standard, adiabatic contraction model for predicting modifications of halo structure due to collisional processes [64–66].

For unstable dark matter, with a lifetime τ_{dm} , a fraction $f(\tau_{dm}, z)$ of unstable dark matter particles will have decayed by redshift z . According to the adiabatic contraction model, the mass enclosed in r_f will be

$$M_f(r_f) = (1 - f(\tau_{dm}, z))M_i(r_i) \quad (19)$$

Inserting Eq. (19) into Eq. (18), the relationship between the initial and final radii is

$$r_f = r_i / (1 - f(\tau_{\text{DDM}}, z)). \quad (20)$$

If we assume that the initial dark matter halos can be well described by NFW profiles, the final mass distribution will be

$$\rho_f(r_f) = \frac{1}{4\pi r_f^2} \frac{dM_f}{dr_f} \quad (21)$$

$$= \frac{(1-f)^2}{4\pi r_f^2} \frac{dM_i}{dr_i} \quad (22)$$

$$= \frac{(1-f)^4 \rho_s}{\left(\frac{(1-f)r_f}{r_s}\right) \left[1 + \frac{(1-f)r_f}{r_s}\right]^2}. \quad (23)$$

We model the initial mass function dn_i/dm and halo bias $b_h(m)$ using the relations of Ref. [67]. This choice is made for convenience because in models with stable dark matter, it satisfies the necessary conditions that the halo model integrals contain all mass and that the clustering of dark matter is unbiased with respect to itself. Some definitions of halo virial radii will be altered by decays. In order to ensure that all mass remains accounted for, we define halos as the mass within virial radii fixed to a definition of 200 times the average density of the Universe in the absence of decays. Thus, virial radii are fixed to be the same as they would be in standard CDM, but halo masses are smaller by a factor of $1 - f(\tau_{\text{DDM}}, z)$. This definition preserves the convenient properties of the bias and mass relations in Ref. [67] and is identical to their halo definition in the absence of dark matter decays.

The new halo mass function at mass M_f is

$$\frac{dn_f(M_f[M_i], z)}{dM_f} = \frac{dn_i(M_i, z)}{dM_i} \left| \frac{dM_i}{dM_f} \right| \quad (24)$$

and

$$b_h(M_f) = b_h(M_i), \quad (25)$$

where the initial and final masses are related via Eq. (19). In other words, we assume the abundance and clustering to follow the abundance and clustering laws for halos of stable dark matter of the corresponding masses. Notice that the abundance of halos of a given contemporary mass M_f is reduced compared to that in a stable dark matter model because the final mass reflects the mass loss due to decays and more massive halos are intrinsically rare. Likewise, halos of final mass M_f are more strongly clustered than their counterparts in stable dark matter scenarios because halo bias is an increasing function of mass (see Ref. [68] for the basic theory of the mass function and bias). The halo density profiles also become shallower as r_s increases and ρ_s decreases when the decay-induced modifications to halo profiles are accounted for.

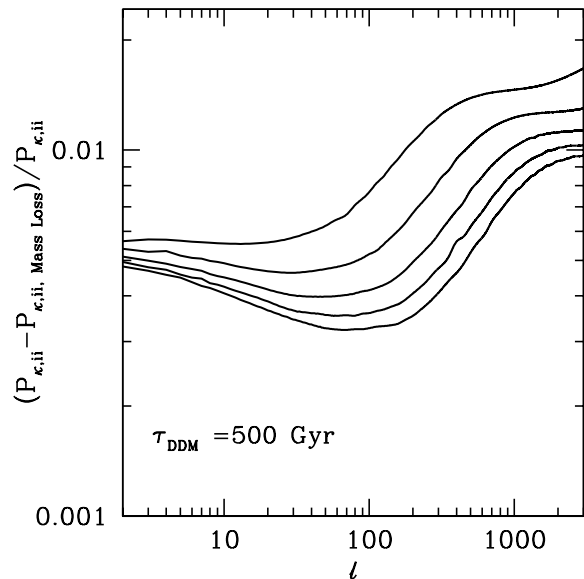


FIG. 1: Fractional difference of shear lensing auto-spectra with and without halo mass loss due to dark matter decay. In this panel, we choose a dark matter lifetime of $\tau = 500$ Gyr for illustrative purposes. From top to bottom, lines are for the auto-spectra of sources in the first tomographic redshift bin ($0 \leq z_p < 0.6$) to the fifth tomographic redshift bin ($2.4 \leq z_p < 3.0$). In this panel, both spectra are computed using a halo model. For comparison, note that the differences between the halo model and the Smith et al. [61] relation can be as much as 20% with the maximum discrepancy near $\ell \sim 1000$.

The reduction in the number of halos and the shallowing of halo profiles reduces lensing power compared to a halo model with no accounting for mass loss. Figure 1 shows a comparison between halo model calculations of lensing power spectra including and neglecting halo mass loss. The greatest changes are at relatively high ℓ ($\ell \gtrsim 300$) and are due to the concentration change which alters the one-halo term [Eq. (16)]. The shift in the mass function and halo bias cause the slight reduction in the two-halo term and power at lower ℓ . As we show in § VI, this additional reduction in power is a distinctive feature that leads to slightly more restrictive bounds on DDM lifetimes.

We emphasize that neither of these approaches have been calibrated in detail on simulations of structure formation in DDM cosmological models. However, we demonstrate that the region of parameter space relevant to forthcoming constraints has $\tau_{\text{DDM}} \gg H_0^{-1}$ (see also [17–20]). This means that little of the DDM will have decayed prior to the present epoch and the boost in signal-to-noise should be something close to that afforded by the nonlinear treatment of standard, stable dark matter. In actuality, *only* a detailed numerical treatment can answer these questions definitively (as Refs. [18, 19] have recently argued). It is our hope that this proof-of-concept paper

will motivate pursuit of large-scale simulations of DDM similar to those being carried out in support of the dark energy constraint program (e.g., [69–71]).

V. FORECASTING METHODS

The Fisher Information Matrix provides a simple estimate of the parameter covariance given data of specified quality. The Fisher matrix has been utilized in numerous, similar contexts in the cosmology literature [43, 48, 60, 72–78], so we give only a brief review of important results and the caveats in our particular application.

The Fisher matrix of observables in Eq. (1), subject to covariance as in Eq. (7), can be written as

$$F_{ij} = \sum_{\ell=\ell_{min}}^{\ell_{max}} (2\ell+1)f_{sky} \sum_{A,B} \frac{\partial P_{\kappa,A}}{\partial p_i} [C^{-1}]_{AB} \frac{\partial P_{\kappa,B}}{\partial p_j} + F_{ij}^P \quad (26)$$

where the indices A and B run over all $N_{\text{TOM}}(N_{\text{TOM}}+1)/2$ spectra and cross spectra, the p_i are the parameters of the model, f_{sky} is the fraction of the sky imaged by the experiment, and $\ell_{min} = 2f_{sky}^{-1/2}$ is the smallest multipole constrained by the experiment. F_{ij}^P is a prior Fisher matrix incorporating previous knowledge of viable regions of parameter space. We set $\ell_{max} = 3000$ in our most ambitious forecasts. On smaller scales (higher ℓ), various assumptions such as the Gaussianity of the lensing field, break down [43, 52–56, 79]. To be conservative, we explore modest priors to each parameter independently, so that $F_{ij}^P = \delta_{ij}/(\sigma_i^P)^2$, where σ_i^P is the 1σ prior on parameter p_i . The forecast, 1σ , marginalized constraint on parameter p_i is $\sigma(p_i) = \sqrt{[F^{-1}]_{ii}}$.

Other than the DDM lifetime τ_{DDM} , we vary six cosmological parameters that we expect to modify weak lensing power spectra at significant levels and to exhibit partial degeneracy with τ_{DDM} . We construct our forecasts for DDM lifetime bounds after marginalizing over the remaining parameters. Our six additional parameters and their fiducial values (in parentheses) are the dark energy density Ω_Λ (0.74), the present-day dark matter density, $\omega_{\text{DM}} = \Omega_{\text{DM}}h^2$ (0.11), the baryon density $\omega_b = \Omega_b h^2$ (0.023), tilt parameter n_s (0.963), the natural logarithm of the primordial curvature perturbation normalization $\ln(\Delta_R^2)$ (−19.94), and the sum of the neutrino masses $\sum_i m_{\nu_i}$ (0.05 eV). This implies a small-scale, low-redshift power spectrum normalization of $\sigma_8 \simeq 0.82$. The optical depth to reionization has a negligible effect on the lensing spectra on scales of interest, so we do not vary it in our analysis. We adopt as our null hypothesis a stable dark matter particle with $\Gamma = 0$. Note that when $\Gamma \neq 0$, there is a *higher* density of dark matter in the past than would be inferred for a stable dark matter particle because we choose our parameter set to describe the contemporary matter density.

We take priors on our cosmological parameters of

$\sigma(\omega_m) = 0.007$, $\sigma(\omega_b) = 1.2 \times 10^{-3}$, $\sigma(\ln \Delta_R^2) = 0.1$, $\sigma(n_s) = 0.015$, and $\sigma(\Omega_\Lambda) = 0.03$. We assume no priors on DDM lifetime or neutrino mass. Our fiducial model is motivated by the WMAP seven-year result and our priors represent marginalized uncertainties on these parameters based on the WMAP seven-year data [80]. These priors are conservative and allow for weaker constraints on DDM than would be expected from future data, where stronger priors may be available. To estimate the potential power of lensing constraints on DDM when stronger cosmological constraints are available, we also explore prior constraints on these parameters at the level expected from the Planck mission¹ using the entire Planck prior Fisher matrix of Ref. [81]. Of course, using published priors from other analyses is not self-consistent because these priors were derived in analyses that assume stable dark matter, but relevant lifetimes the dark matter decays should cause only subtle alterations to the cosmic microwave background anisotropy spectrum so this analysis should approximate a self-consistent simultaneous analysis of all data.

In some cases, we will estimate *nonlinear* power spectra in models with significant neutrino masses. In such cases, we follow the empirical prescription established in previous studies (e.g., Refs. [77, 82, 83]) and take

$$P_m(k) = \left[f_\nu \sqrt{P_\nu^{\text{lin}}(k)} + f_{b+\text{DM}} \sqrt{P_{b+\text{DM}}^{\text{NL}}(k)} \right]^2 \quad (27)$$

where

$$f_\nu = \frac{\Omega_\nu}{\Omega_m}, \quad (28a)$$

$$f_{b+\text{DM}} = \frac{\Omega_{\text{DM}} + \Omega_b}{\Omega_m}, \quad (28b)$$

$P_\nu^{\text{lin}}(k)$ is the linear power spectrum of neutrinos, and $P_{b+\text{DM}}^{\text{NL}}(k)$ is the nonlinear power spectrum evaluated for baryons and dark matter only. Again, our adoption of this prescription may induce errors in our calculation and only a large-scale numerical simulation program can test this assumption.

We explore possible constraints from a variety of forthcoming data sets. We consider the Dark Energy Survey (DES)² as a near-term imaging survey that could provide requisite data for this test. We model DES by taking a fractional sky coverage of $f_{sky} = 0.12$ and with $\bar{n} = 15/\text{arcmin}^2$. Second, we consider a comparably narrow, deep imaging survey as may be carried out from a space-based platform, such as a Supernova Acceleration Probe-like implementation of a Joint Dark Energy Mission (JDEM)^{3,4} or the National Academy of Science's

¹ <http://www.esa.int/planck>

² <http://www.darkenergysurvey.org>

³ <http://universe.nasa.gov/program/probes/jdem>

⁴ <http://snap.lbl.gov/>

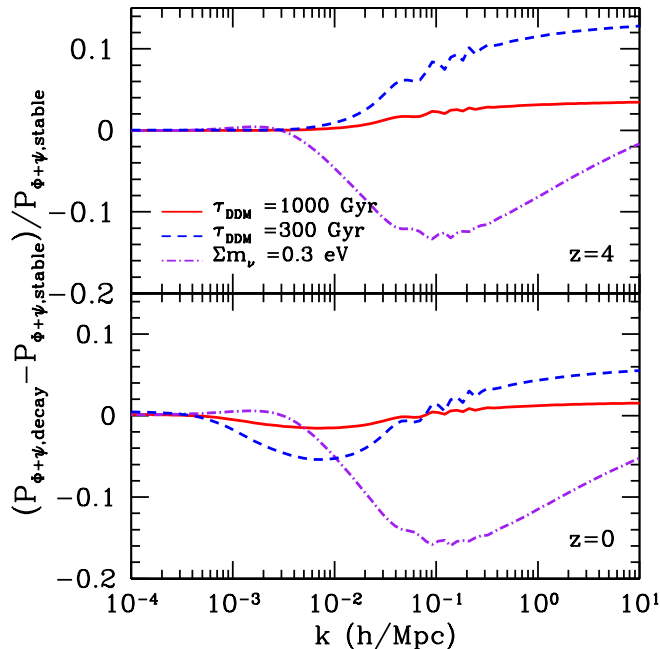


FIG. 2: Relative difference in the linear potential power spectra between DDM and stable dark matter models at $z = 4$ (top) and $z = 0$ (bottom). The *solid* lines show a model with $\tau_{\text{DDM}} = 10^3$ Gyr while the *dashed* lines have $\tau_{\text{DDM}} = 300$ Gyr. The *dash-dotted* lines show the influence of a non-negligible neutrino mass with $\sum_i m_{\nu_i} = 0.3$ eV.

Astronomy and Astrophysics Decadal Survey suggestion of a Wide Field Infrared Space Telescope (WFIRST)⁵. We refer to such a survey as a “Deep” survey and model it with $f_{\text{sky}} = 0.05$ and $\bar{n} = 100/\text{arcmin}^2$. Lastly, we consider a class of future “Wide” surveys as may be carried out by the Large Synoptic Survey Telescope (LSST)⁶ [38] or Euclid⁷ [39]. We model these Wide surveys with $f_{\text{sky}} = 0.5$ and $\bar{n} = 50/\text{arcmin}^2$. In all cases, we take $\sqrt{\langle \gamma^2 \rangle} = 0.2$ and assume particular shape measurement errors from each experiment are encapsulated in their effective number densities, in accord with recent conventional practice in this regard. Our results are relatively insensitive to number density because shot noise does not dominate cosmic variance on the scales we consider for any of the experimental parameters we consider.

The Fisher matrix is valuable because it greatly reduces the computational effort necessary to forecast constraints from forthcoming experimental data. However, the Fisher matrix formalism has important drawbacks. First, the Fisher matrix only characterizes parameter degeneracies locally about the fiducial model. Second, the

Fisher matrix formalism cannot formally be applied to parameters near physical limits in their parameter values. In such cases, a Fisher approach allows for parameter degeneracies that extend into the forbidden region of the parameter space and should not be permitted on physical grounds. This additional degeneracy tends to cause under estimates of constraints that may be realized from a more detailed analysis. An example of this is neutrino mass. The Fisher matrix has been utilized to constrain neutrino mass and empirically Fisher matrix projections for neutrino mass constraints have been shown to match well direct searches of parameter space (e.g., [77, 82–85]) To verify our Fisher matrix results, we have performed several direct searches of subspaces of our full parameter space (limited by computational cost) to constrain DDM lifetime. Generally, we find the marginalized Fisher constraints to be only slightly less constraining than the direct search results and we present an example of this in the following section. The computational cost of a full parameter search seems unwarranted given the theoretical limitations discussed in § III.

VI. RESULTS

A. Weak Lensing Power Spectra

Weak lensing power spectra are altered by DDM in two respects. First, the power spectra for potential and density fluctuations are altered in a scale-dependent way. At early epochs, when the matter density is higher in the DDM models than in standard Λ CDM, potential and density fluctuations are larger because the epoch of matter-radiation equality occurs earlier. We have verified that our constraints are insensitive to the epoch at which we normalize the matter density. At late times, DDM decays suppress density and potential fluctuations. We show this dependence of potential fluctuations on DDM lifetime in Figure 2. Notice that models of unstable dark matter have greater $P_{\Psi-\Phi}(k)$ on scales $k \gtrsim 10^{-2} h \text{ Mpc}^{-1}$ at high redshift, but this power is suppressed on subhorizon ($k \gtrsim 10^{-3} h \text{ Mpc}^{-1}$) at lower redshifts. The strong scale dependence in potential power spectra at scales of order $k \sim 0.05 h \text{ Mpc}^{-1}$ should be present in convergence spectra projected on multipoles $\ell \sim k D_A(z=1) \sim 150$ ($z=1$ is the median redshift of lensed sources in our model surveys). The different redshift dependence of DDM, which results in greater suppression of power with decreasing redshift, compared to neutrino mass-induced power suppression allows the two to be disentangled.

The observed strength of gravitational lensing also has a dependence upon geometry, so differences in angular diameter distance may lead to modified lensing power spectra. These geometrical differences provide the bulk of the information with which lensing can constrain dark energy [86, 87] and the angular diameter distance to the last-scattering surface has been used to constrain decaying *dark matter* in previous studies [17, 20]. In princi-

⁵ http://sites.nationalacademies.org/bpa/BPA_049810

⁶ <http://www.lsst.org>

⁷ <http://sci.esa.int/euclid>

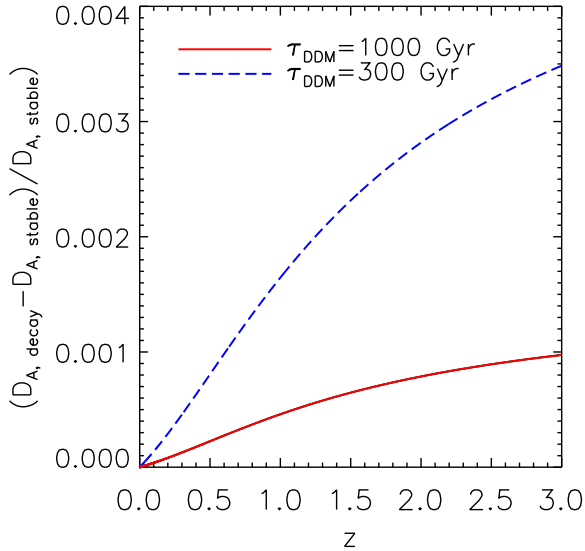


FIG. 3: Relative differences in comoving angular diameter distance between models with DDM and stable dark matter as a function of scale factor. The *solid* line represents a model with $\tau_{\text{DDM}} = 10^3$ Gyr and the *dashed* line shows a model with $\tau_{\text{DDM}} = 300$ Gyr.

ple, the distance-redshift relation in decaying dark matter models can be mimicked by dark energy with a variable equation of state [88]. We show in Fig. 3 a comparison of the angular diameter distance in DDM models. Fig. 3 demonstrates the angular diameter distances are modified at levels that are small compared to the relative potential fluctuations shown in Fig. 2. As a consequence, we find that DDM constraints are based mainly on the scale-dependent potential fluctuation modifications, rather than on the modified distance scale which is the primary driver of *dark energy* constraints.

These changes manifest in a scale- and redshift-dependent shift in observable convergence power spectra. We show examples of the shift in the convergence power spectra in models of unstable dark matter in Figure 4. Notice the strong scale dependence on multipoles of a few hundred. On smaller scales, the net effect is an overall change to the level of the convergence power, with only a weak scale dependence. This is one reason that we anticipate that we may be able to utilize the methods of Smith et al. [61] or Peter [18] to approximate the constraining power of weak lensing surveys when nonlinear evolution is included.

B. Forecast Constraints on DDM Lifetimes

As a first attempt to estimate the power of weak lensing to constrain DDM, we examine models in which we consider only the linear evolution of potential and density fluctuations. We consider taking the maximum multipole that we may observe as high as $\ell_{\text{max}} = 3000$; however,

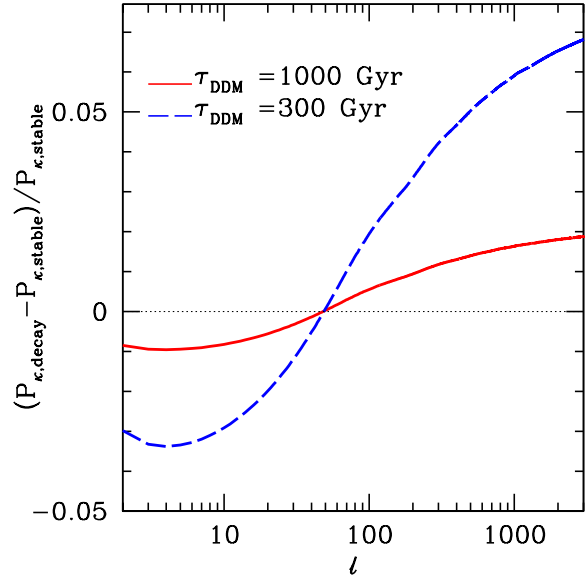


FIG. 4: Relative modification to linear lensing convergence power spectra caused by DDM. The lines show the convergence power spectra for galaxies in our third redshift bin (galaxies with photometric redshifts $1.2 \leq z_p < 1.8$) in models with finite τ_{DDM} compared to a model with stable dark matter. The *solid* line shows the power spectrum residual in a model with $\tau_{\text{DDM}} = 1000$ Gyr, and the *dashed* line shows the same power spectrum residual with $\tau_{\text{DDM}} = 300$ Gyr.

for multipoles larger than $\ell \gtrsim 300$ nonlinear effects will be very important [43] (also, see Fig. 1). Therefore, we also consider taking $\ell_{\text{max}} = 300$ so that we consider only those scales for which linear perturbative evolution may be valid. In this case, our theoretical methods are applicable and forthcoming weak lensing constraints should do *at least* this well.

In our most ambitious forecasts, we *assume* that we can use the nonlinear formula of Smith et al. [61] or the halo model to estimate the boost in signal that nonlinear evolution may provide for weak lensing constraints on DDM. These approaches toward nonlinear corrections are not entirely self-consistent, but may serve as an indicator of what could be achieved if a numerical simulation effort addressed nonlinear evolution in DDM robustly.

We summarize our primary results for the upper limits that may be set on the DDM decay rate Γ , by weak lensing measurements in Table I. The limits in this table have been marginalized over all other cosmological parameters, including neutrino masses. We computed the results in the upper portion of Table I using contemporary priors on other cosmological parameters. Results below the middle dividing line of Table I were computed with prior constraints on cosmology at levels expected from the Planck CMB mission and are labeled with a “PP.” Different lines in Table I show results using different model power spectra. The options are the linearly-evolved power spectrum only, results correcting for non-

TABLE I: Forecast 68% marginalized limits on dark matter decay rates from weak lensing surveys under several assumptions. The limits are in units Γ/H_0 , where $H_0 = 72$ km/s/Mpc. Constraints are shown for “Linear” power spectra, “Smith et al.” nonlinear corrections, “Halo Model” nonlinear corrections, and “Modified Halo Model” nonlinear corrections that account for mass loss as in Ref. [18]. The abbreviation “PP” stands for Planck priors.

Experiment	DES	Deep	Wide
Linear, $\ell_{max} = 3000$	0.07	0.06	0.046
Linear, $\ell_{max} = 300$	0.08	0.09	0.057
Smith et al, $\ell_{max} = 3000$	0.03	0.02	0.008
Smith et al, $\ell_{max} = 300$	0.06	0.05	0.029
Halo Model, $\ell_{max} = 3000$,	0.03	0.02	0.010
Modified Halo Model, $\ell_{max} = 3000$,	0.02	0.02	0.008
Linear, $\ell_{max} = 3000$, PP	0.03	0.03	0.016
Linear, $\ell_{max} = 300$, PP	0.06	0.07	0.026
Smith et al, $\ell_{max} = 3000$, PP	0.02	0.01	0.006
Smith et al, $\ell_{max} = 300$, PP	0.05	0.05	0.018
Halo Model, $\ell_{max} = 3000$, PP	0.02	0.02	0.007
Modified Halo Model, $\ell_{max} = 3000$, PP	0.02	0.01	0.006

linear evolution using the Smith et al. [61] formula, nonlinear power results using the halo model, and nonlinear power using the halo model modified to account for the loss of mass within halos (following Ref. [18]). In each case, we consider both restricting to linear scales taking $\ell_{max} = 300$ and using nonlinear information with $\ell_{max} = 3000$ to constrain decaying dark matter.

Constraints that exploit only linear scales are already promising. A DES, a Deep JDEM/WFIRST-like survey, or a Wide LSST- or Euclid-like survey should constrain the DDM lifetime at the level of $\tau_{\text{DDM}} = \Gamma^{-1} \gtrsim 13H_0^{-1}$, $12H_0^{-1}$, and $18H_0^{-1}$ with contemporary priors on other cosmological parameters. These results are already comparable to contemporary, model-independent constraints on unstable dark matter [16–21] and do not require detailed calibration of nonlinear structure growth or ambitious priors on other cosmological parameters ($\ln \Delta_R^2$ in particular). It seems reasonable then, that weak gravitational lensing will provide, at minimum, a complementary, model-independent technique to constrain DDM that is competitive with other, existing techniques.

If we interpret the other entries in Table I as possible limits that may be achieved if the necessary nonlinear evolution in models of DDM can be calibrated, then the results become much more interesting. Using contemporary priors, the limits range between $\tau_{\text{DDM}} \gtrsim 33H_0^{-1}$ and $\tau_{\text{DDM}} \gtrsim 43H_0^{-1}$ for DES, $\tau_{\text{DDM}} \gtrsim 48H_0^{-1}$ and $\tau_{\text{DDM}} \gtrsim 66H_0^{-1}$ for our Deep survey, and $\tau_{\text{DDM}} \gtrsim 100H_0^{-1}$ and $\tau_{\text{DDM}} \gtrsim 125H_0^{-1}$ for our Wide survey. The variation between the lower values and higher values exhibits the range of possible constraints estimated using different nonlinear structure formation

prescriptions. In all cases, the standard halo model gives the poorest constraint and the halo model modified to account for mass loss as the dark matter decays, as described in § IV, gives the most stringent constraint. The ability to exploit nonlinear power enables weak lensing to constrain unstable dark matter more stringently than contemporary methods using contemporary priors.

Our most ambitious constraints come from assuming that Planck constraints on cosmological parameters other than Γ are available and that nonlinear structure formation can be calibrated sufficiently to make full use of weak lensing data on nonlinear scales alongside Planck priors. These constraints are listed in the lower section of Table I. In this most ambitious scenario, the lensing constraints on unstable dark matter are $\tau_{\text{DDM}} \gtrsim 50H_0^{-1}$ for DES, $\tau_{\text{DDM}} \gtrsim 100H_0^{-1}$ for a Deep, JDEM/WFIRST-like survey, and $\tau_{\text{DDM}} \gtrsim 170H_0^{-1}$ for a Wide, LSST- or Euclid-like survey. Under these circumstances, weak lensing will provide the most stringent, model-independent constraints on the decay lifetime of the dark matter particle.

Numerous observational systematics need to be controlled for these instruments to achieve their statistical limitations and the theory on nonlinear structure growth in models with DDM must also be computed more rigorously. However, our ambitious forecast limits exceed contemporary bounds on dark matter with invisible decay channels significantly, so that even if observational or theoretical systematics persist, weak lensing may yet provide the strongest limits on DDM. This opportunity (along with the related considerations in [16, 18, 19]) provides a strong argument for a large-scale computational program to study the nonlinear evolution of density fluctuations in models with DDM.

We conclude our results section, by addressing two remaining outstanding issues. First, the most obvious standard cosmological parameters that we may suspect to be degenerate with DDM are neutrino mass and the normalization of the matter power spectrum on large scales. Much of the constraining power of lensing comes from comparing contemporary potential fluctuations to those measured using the CMB at high redshift whereas significant neutrino mass also gives rise to scale-dependent suppression of the potential power spectra. Figure 2 provides anecdotal evidence that neutrino mass and DDM should not be so degenerate as to destroy constraining power because they change the linearly-evolved potential spectra in different ways. Most importantly, the effect of DDM is strongly redshift dependent. Figure 5 shows projected confidence contours projected onto two-dimensional subspaces of our parameter space. Figure 5 shows that significant degeneracies do exist when only contemporary priors are used, and Planck priors suffice to break most of these degeneracies, leaving a slight degeneracy with neutrino mass as the most prominent. In the limit of a known neutrino mass (perhaps constrained by laboratory experiments), our constraints on DDM lifetimes improve by roughly $\sim 25\%$, yielding a best-case constraint from a WIDE survey of $\tau_{\text{DDM}} \gtrsim 210H_0^{-1}$.

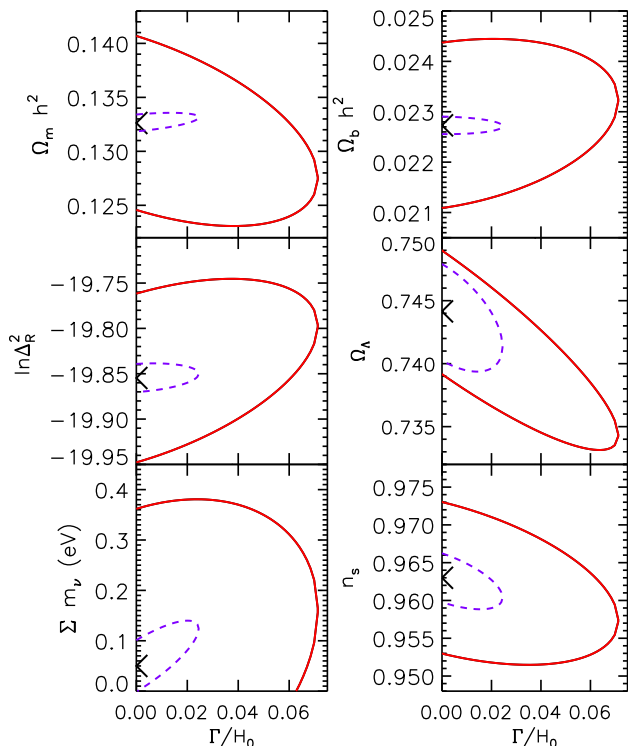


FIG. 5: Marginalized, 1σ constraint contours for dark matter decay rate against other varying cosmological parameters in our model. In this illustrative example, we show contours from our linear power spectrum, $\ell_{\max} = 300$, Wide survey calculations. The outer contours were computed using our contemporary priors while the inner contours were computed assuming Planck-level priors. This example is useful because degeneracies are most significant in the linear power spectrum calculations. Notice that the degeneracy between dark matter lifetime and neutrino mass is relatively insignificant for contemporary priors, but is the most important remaining degeneracy with Planck prior constraints. The crosses designate fiducial parameter values.

Finally, we have performed several direct searches through reduced cosmological and DDM parameter space to support our use of the Fisher matrix approach in the full parameter space. The need to reduce the parameter space in direct searches is to limit computational effort. At present, with the nonlinear evolution in DDM models still uncertain, it does not seem fruitful to spend significant computational effort on forecasting. In a simple, linear power model in which we scan the parameter space of Γ , ω_m , ω_b , $\ln(\Delta_R^2)$, and Ω_Λ , we find that our direct search decay rate bounds agree with the Fisher estimates to within $\sim 20\%$ for our Wide survey. Moreover, the Fisher estimates are typically *weaker* than the projected direct search limits, largely because the Fisher matrix allows for degeneracies among parameters that would not be permitted on physical grounds. Our Fisher matrix forecasts are insensitive to the fiducial value of Γ , so long as the DDM lifetime is significantly larger than a Hubble time.

VII. CONCLUSIONS

We examined the utility of forthcoming, large-scale imaging surveys to constrain the lifetime of dark matter decay into light daughter particles. Decaying dark matter can be disentangled from dark energy, because its primary observational signature is to reduce the potential fluctuation power spectrum, while dark energy is primarily constrained by geometric effects [86, 87]. DDM can be distinguished from massive neutrinos because the suppression of power is a strong function of redshift. Assuming a null hypothesis of stable dark matter, we found that utilizing only the information from linear scales ($\ell \lesssim 300$) may suffice to place competitive limits on dark matter decay rates. Our linear-only, conservative forecast limits are $\Gamma^{-1} \gtrsim 13H_0^{-1}$ for DES, $\Gamma^{-1} \gtrsim 12H_0^{-1}$ for a Deep JDEM/WFIRST-like survey, and $\Gamma^{-1} \gtrsim 18H_0^{-1}$ for a Wide LSST- or Euclid-like survey. The DES limit is slightly weaker than the best contemporary constraints [17, 18, 20, 21], while the Wide limit is stronger. The constraint comes largely from a scale- and redshift-dependent reduction in convergence power. This indicates that without any further theoretical development, such instruments should provide competitive, complementary limits on unstable dark matter.

In practice, lensing surveys will likely measure convergence spectra over a wide range of scales where nonlinear evolution is important to model ($\ell \sim 10^3$). The improved signal-to-noise from measurement on these scales should dramatically improve upon our conservative forecasts. Assuming that we can use a halo model to map our linear spectra onto nonlinear spectra, we forecast limits that may be as stringent as $\Gamma^{-1} \gtrsim 50H_0^{-1}$ for DES, $\Gamma^{-1} \gtrsim 100H_0^{-1}$ for a Deep JDEM/WFIRST-like survey, and $\Gamma^{-1} \gtrsim 170H_0^{-1}$ for a Wide LSST- or Euclid-like survey when combining with Planck satellite data. These forecasts are more restrictive than constraints available via other means.

Of course, these more aggressive limit forecasts come with caveats. Developing surveys must control numerous nontrivial systematics to bring their lensing programs to fruition and nonlinear evolution in models of DDM has not been explored well theoretically. Weak lensing systematics will be explored in support of the well-established goal of using lensing to constrain dark energy. A few groups have performed simulations with DDM models to understand its effect on dark matter halos and galaxy formation [19, 89]. However the number of samples and the simulated halo mass range are not yet sufficient to provide an adequate nonlinear fit to matter power spectra. It is our hope that the opportunity to limit unstable dark matter using information on nonlinear scales (see also [18]) will motivate researchers to explore nonlinear structure formation in models of unstable dark matter. If this can be done, it may be possible to limit the dark matter lifetime to be greater than hundreds of Hubble times. Furthermore, it would worth-

while to extend such calculations to models with small parent-daughter mass splittings. Such models introduce an additional parameter (the mass splitting) that determines the recoil energies of the particles after decay. Such recoils may alter nonlinear structure at a level detectable with lensing data [18, 19]. The future is promising for limiting the instability of dark matter using forthcoming, large-scale astronomical surveys.

Acknowledgments

We are grateful to Mickey Abbott, Dan Boyanovsky, James Bullock, Andrew Hearin, Wayne Hu, Dragan

Huterer, Arthur Kosowsky, Jeff Newman, Annika Peter, and Chris Purcell for useful comments and discussions. This work was funded by the University of Pittsburgh, the National Science Foundation through grant PHY 0968888. We thank Uros Seljak and Mathias Zaldarriaga for use of the publicly-available CMBFAST code. This work made use of the NASA Astrophysics Data System.

-
- [1] G. Jungman, M. Kamionkowski, and K. Griest, *Phys. Rep.* **267**, 195 (1996), arXiv:hep-ph/9506380.
- [2] K. Griest and M. Kamionkowski, *Phys. Rep.* **333**, 167 (2000).
- [3] G. Bertone, D. Hooper, and J. Silk, *Phys. Rep.* **405**, 279 (2005), arXiv:hep-ph/0404175.
- [4] J. Cooley and I. the CDMS Collaboration, *Journal of Physics Conference Series* **203**, 012004 (2010), arXiv:0912.1601.
- [5] J. Angle, E. Aprile, F. Arneodo, L. Baudis, A. Bernstein, A. Bolozdynya, P. Brusov, L. C. C. Coelho, C. E. Dahl, L. Deviveiros, et al., *Physical Review Letters* **100**, 021303 (2008), arXiv:0706.0039.
- [6] R. Bernabei, P. Belli, F. Cappella, R. Cerulli, C. J. Dai, A. d'Angelo, H. L. He, A. Incicchitti, H. H. Kuang, X. H. Ma, et al., arXiv:1002.1028 (2010).
- [7] C. E. Aalseth, P. S. Barbeau, N. S. Bowden, B. Cabrera-Palmer, J. Colaresi, J. I. Collar, S. Dazeley, P. de Lurgio, G. Drake, J. E. Fast, et al., ArXiv e-prints (2010), arXiv:1002.4703.
- [8] E. Aprile and XENON Collaboration, *Journal of Physics Conference Series* **203**, 012005 (2010).
- [9] R. Abbasi et al., *Physical Review Letters* **102**, 201302 (2009), arXiv:0902.2460.
- [10] V. Vitale, A. Morselli, and for the Fermi/LAT Collaboration, arXiv:0912.3828 (2009).
- [11] E. Komatsu, J. Dunkley, M. R. Nolte, C. L. Bennett, B. Gold, G. Hinshaw, N. Jarosik, D. Larson, M. Limon, L. Page, et al., *Astrophys. J. Suppl. Ser.* **180**, 330 (2009), arXiv:0803.0547.
- [12] K. N. Abazajian, M. Markevitch, S. M. Koushiappas, and R. C. Hickox, *Phys. Rev. D* **75**, 063511 (2007), arXiv:astro-ph/0611144.
- [13] S. W. Randall, M. Markevitch, D. Clowe, A. H. Gonzalez, and M. Bradač, *Astrophys. J.* **679**, 1173 (2008), arXiv:0704.0261.
- [14] A. Boyarsky, J. Lesgourgues, O. Ruchayskiy, and M. Viel, *Journal of Cosmology and Astro-Particle Physics* **5**, 12 (2009), arXiv:0812.0010.
- [15] M. Kaplinghat, R. E. Lopez, S. Dodelson, and R. J. Scherrer, *Phys. Rev. D* **60**, 123508 (1999), arXiv:astro-ph/9907388.
- [16] K. Ichiki, M. Oguri, and K. Takahashi, *Physical Review Letters* **93**, 071302 (2004), arXiv:astro-ph/0403164.
- [17] Y. Gong and X. Chen, *Phys. Rev. D* **77**, 023009 (2008), arXiv:0802.2296.
- [18] A. H. G. Peter, ArXiv e-prints (2010), arXiv:1001.3870.
- [19] A. H. G. Peter, C. E. Moody, and M. Kamionkowski, ArXiv e-prints (2010), arXiv:1003.0419.
- [20] A. R. Zentner and T. P. Walker, *Phys. Rev. D* **65**, 063506 (2002), arXiv:astro-ph/0110533.
- [21] S. De Lope Amigo, W. Cheung, Z. Huang, and S. Ng, *ArXiv Astrophysics e-prints* (2009), arXiv:0812.4016.
- [22] M. Oguri, K. Takahashi, H. Ohno, and K. Kotake, *Astrophys. J.* **597**, 645 (2003), arXiv:astro-ph/0306020.
- [23] D. Puetzfeld and X. Chen, *Classical and Quantum Gravity* **21**, 2703 (2004), arXiv:gr-qc/0402026.
- [24] S. Palomares-Ruiz, *Physics Letters B* **665**, 50 (2008), arXiv:0712.1937.
- [25] F. Borzumati, T. Bringmann, and P. Ullio, *Phys. Rev. D* **77**, 063514 (2008), arXiv:hep-ph/0701007.
- [26] X. Chen and M. Kamionkowski, *Phys. Rev. D* **70**, 043502 (2004), arXiv:astro-ph/0310473.
- [27] S. H. Hansen and Z. Haiman, *Astrophys. J.* **600**, 26 (2004), arXiv:astro-ph/0305126.
- [28] M. Mapelli, A. Ferrara, and E. Pierpaoli, *Mon. Not. R. Astron. Soc.* **369**, 1719 (2006), arXiv:astro-ph/0603237.
- [29] L. Zhang, X. Chen, M. Kamionkowski, Z. Si, and Z. Zheng, *Phys. Rev. D* **76**, 061301 (2007), 0704.2444.
- [30] H. Yüksel and M. D. Kistler, *Phys. Rev. D* **78**, 023502 (2008), arXiv:0711.2906.
- [31] B. Feldstein and A. L. Fitzpatrick, arXiv:1003.5662 (2010).
- [32] K. Takahashi, M. Oguri, and K. Ichiki, *Mon. Not. R. Astron. Soc.* **352**, 311 (2004), arXiv:astro-ph/0312358.
- [33] J. L. Feng, H. Tu, and H. Yu, *Journal of Cosmology and Astro-Particle Physics* **10**, 43 (2008), arXiv:0808.2318.
- [34] J. L. Feng, M. Kaplinghat, H. Tu, and H. Yu, *Journal of Cosmology and Astro-Particle Physics* **7**, 4 (2009), arXiv:0905.3039.
- [35] L. Ackerman, M. R. Buckley, S. M. Carroll, and M. Kamionkowski, *Phys. Rev. D* **79**, 023519 (2009), arXiv:0810.5126.
- [36] A. Falkowski, J. Juknevič, and J. Shelton, arXiv:0908.1790 (2009).
- [37] D. B. Kaplan, M. A. Luty, and K. M. Zurek, *Phys. Rev. D* **79**, 115016 (2009).
- [38] L. S. Collaborations, arXiv:0912.0201 (2009).

- [39] A. Refregier, A. Amara, T. D. Kitching, A. Rassat, R. Scaramella, J. Weller, and f. t. Euclid Imaging Consortium, ArXiv:1001.0061 (2010).
- [40] F. Schmidt, Phys. Rev. D **78**, 043002 (2008), 0805.4812.
- [41] Z. Ma, W. Hu, and D. Huterer, Astrophys. J. **636**, 21 (2006), astro-ph/0506614.
- [42] D. Huterer, arXiv:1001.1758 (2010).
- [43] A. R. Zentner, D. H. Rudd, and W. Hu, Phys. Rev. D **77**, 043507 (2008), arXiv:0709.4029.
- [44] C. Ma and E. Bertschinger, Astrophys. J. **455**, 7 (1995), arXiv:astro-ph/9506072.
- [45] I. Smail, D. W. Hogg, L. Yan, and J. G. Cohen, Astrophys. J. Lett. **449**, L105+ (1995), arXiv:astro-ph/9506095.
- [46] I. Smail, R. S. Ellis, M. J. Fitchett, and A. C. Edge, Mon. Not. R. Astron. Soc. **273**, 277 (1995), arXiv:astro-ph/9402049.
- [47] J. A. Newman, Astrophys. J. **684**, 88 (2008), arXiv:0805.1409.
- [48] G. Bernstein and D. Huterer, Mon. Not. R. Astron. Soc. **401**, 1399 (2010), arXiv:0902.2782.
- [49] A. P. Hearin, A. R. Zentner, Z. Ma, and D. Huterer, ArXiv e-prints (2010), arXiv:1002.3383.
- [50] R. Massey, J. Rhodes, A. Refregier, J. Albert, D. Bacon, G. Bernstein, R. Ellis, B. Jain, T. McKay, S. Perlmutter, et al., Astron. J. **127**, 3089 (2004), arXiv:astro-ph/0304418.
- [51] M. M. Kasliwal, R. Massey, R. S. Ellis, S. Miyazaki, and J. Rhodes, Astrophys. J. **684**, 34 (2008), 0710.3588.
- [52] M. White and W. Hu, Astrophys. J. **537**, 1 (2000).
- [53] A. Cooray and W. Hu, Astrophys. J. **554**, 56 (2001), astro-ph/0012087.
- [54] C. Vale and M. White, Apj **592**, 699 (2003).
- [55] S. Dodelson, C. Shapiro, and M. White, Phys. Rev. D **73**, 023009 (2006), arXiv:astro-ph/0508296.
- [56] E. Semboloni, L. van Waerbeke, C. Heymans, T. Hamana, S. Colombi, M. White, and Y. Mellier, Mon. Not. R. Astron. Soc. **375**, L6 (2007), arXiv:astro-ph/0606648.
- [57] U. Seljak and M. Zaldarriaga, Astrophys. J. **469**, 437 (1996), arXiv:astro-ph/9603033.
- [58] A. Cooray, W. Hu, and J. Miralda-Escude, Astrophys. J. **535**, L9 (2000), astro-ph/0003205.
- [59] M. White, Astroparticle Physics **22**, 211 (2004), astro-ph/0405593.
- [60] D. Huterer and M. Takada, Astroparticle Physics **23**, 369 (2005), astro-ph/0412142.
- [61] R. E. Smith, J. A. Peacock, A. Jenkins, S. D. M. White, C. S. Frenk, F. R. Pearce, P. A. Thomas, G. Efstathiou, and H. M. P. Couchman, Mon. Not. R. Astron. Soc. **341**, 1311 (2003), astro-ph/0207664.
- [62] A. Cooray and R. Sheth, Phys. Rep. **372**, 1 (2002).
- [63] J. F. Navarro, C. S. Frenk, and S. D. M. White, Astrophys. J. **490**, 493 (1997), astro-ph/9611107.
- [64] Y. Zeldovich, A. A. Klypin, M. Y. Khlopov, and V. M. Chechetkin, Soviet J. Nucl. Phys. **31**, 664 (1980).
- [65] G. R. Blumenthal, S. M. Faber, R. Flores, and J. R. Primack, Astrophys. J. **301**, 27 (1986).
- [66] O. Y. Gnedin, A. V. Kravtsov, A. A. Klypin, and D. Nagai, Astrophys. J. **616**, 16 (2004), astro-ph/0406247.
- [67] R. K. Sheth and G. Tormen, Mon. Not. R. Astron. Soc. **308**, 119 (1999), astro-ph/9901122.
- [68] A. R. Zentner, International Journal of Modern Physics D **16**, 763 (2007), arXiv:astro-ph/0611454.
- [69] K. Heitmann, P. M. Ricker, M. S. Warren, and S. Habib, Astrophys. J. Suppl. Ser. **160**, 28 (2005), astro-ph/0411795.
- [70] K. Heitmann, M. White, C. Wagner, S. Habib, and D. Higdon, ArXiv:0812.1052 (2008).
- [71] K. Heitmann, D. Higdon, M. White, S. Habib, B. J. Williams, and C. Wagner, ArXiv:0902.0429 (2009).
- [72] G. Jungman, M. Kamionkowski, A. Kosowsky, and D. N. Spergel, Phys. Rev. D **54**, 1332 (1996), arXiv:astro-ph/9512139.
- [73] M. Tegmark, A. N. Taylor, and A. F. Heavens, Astrophys. J. **480**, 22 (1997), arXiv:astro-ph/9603021.
- [74] U. Seljak, Astrophys. J. **482**, 6 (1997), arXiv:astro-ph/9608131.
- [75] W. Hu, Astrophys. J. Lett. **522**, L21 (1999), astro-ph/9904153.
- [76] A. Kosowsky, M. Milosavljevic, and R. Jimenez, Phys. Rev. D **66**, 063007 (2002), arXiv:astro-ph/0206014.
- [77] T. D. Kitching, A. F. Heavens, L. Verde, P. Serra, and A. Melchiorri, Phys. Rev. D **77**, 103008 (2008), arXiv:0801.4565.
- [78] A. H. G. Peter, ArXiv e-prints (2009), arXiv:0910.4765.
- [79] D. H. Rudd, A. R. Zentner, and A. V. Kravtsov, Astrophys. J. **672**, 19 (2008), arXiv:astro-ph/0703741.
- [80] E. Komatsu, K. M. Smith, J. Dunkley, C. L. Bennett, B. Gold, G. Hinshaw, N. Jarosik, D. Larson, M. R. Nolta, L. Page, et al., ArXiv e-prints (2010), arXiv:1001.4538.
- [81] W. Hu, D. Huterer, and K. M. Smith, Astrophys. J. Lett. **650**, L13 (2006), arXiv:astro-ph/0607316.
- [82] S. Hannestad, H. Tu, and Y. Y. Wong, Journal of Cosmology and Astro-Particle Physics **6**, 25 (2006), arXiv:astro-ph/0603019.
- [83] K. Ichiki, M. Takada, and T. Takahashi, Phys. Rev. D **79**, 023520 (2009), arXiv:0810.4921.
- [84] F. de Bernardis, T. D. Kitching, A. Heavens, and A. Melchiorri, Phys. Rev. D **80**, 123509 (2009), arXiv:0907.1917.
- [85] I. Debono, A. Rassat, A. Réfrégier, A. Amara, and T. D. Kitching, Mon. Not. R. Astron. Soc. pp. 249+ (2010), arXiv:0911.3448.
- [86] H. Zhan and L. Knox, ArXiv Astrophysics e-prints (2006), arXiv:astro-ph/0611159.
- [87] A. P. Hearin and A. R. Zentner, Journal of Cosmology and Astro-Particle Physics **4**, 32 (2009), arXiv:0904.3334.
- [88] S. Dutta and R. J. Scherrer, Phys. Rev. D **82**, 043526 (2010), 1004.3295.
- [89] F. Ferrer, C. Nipoti, and S. Etori, Phys. Rev. D **80**, 061303 (2009), arXiv:0905.3161.